

# M1-67 and RCW 58: nebulae around WN8h stars formed through CE evolution



P. Jiménez-Hernández<sup>1</sup>,  
S. J. Arthur<sup>1</sup>, J. A. Toalá<sup>1</sup> & A. P. Marston<sup>2</sup>  
<sup>1</sup>Instituto de Radioastronomía y Astrofísica, UNAM  
<sup>2</sup>European Space Astronomy Centre, ESA

p.jimenez@irya.unam.mx



## Outline

Some late-type WNh Wolf-Rayet (WR) stars are surrounded by clumpy or irregular ejecta nebulae, suggesting a violent mass-loss episode as their origin. The study of WR nebulae properties can provide information of the mass-loss history of massive stars in the late stages of their evolution. The WNh stars are WR N-rich stars characterized by H emission lines. In particular, we are looking at the evolution of the dust properties in WR nebulae around WN8h stars in order to understand the post-main sequence evolution of these stars.

## Models

The photoionization code Cloudy [1] allows us to treat the interaction between the UV flux from the central star and the nebular gas and dust consistently. For the spectrum of the central stars we used PoWR stellar atmosphere models [2] (see Fig. 3). Cloudy also needs the density profiles of nebular material and the dust grains properties. In our models we include only spherical silicate grains.

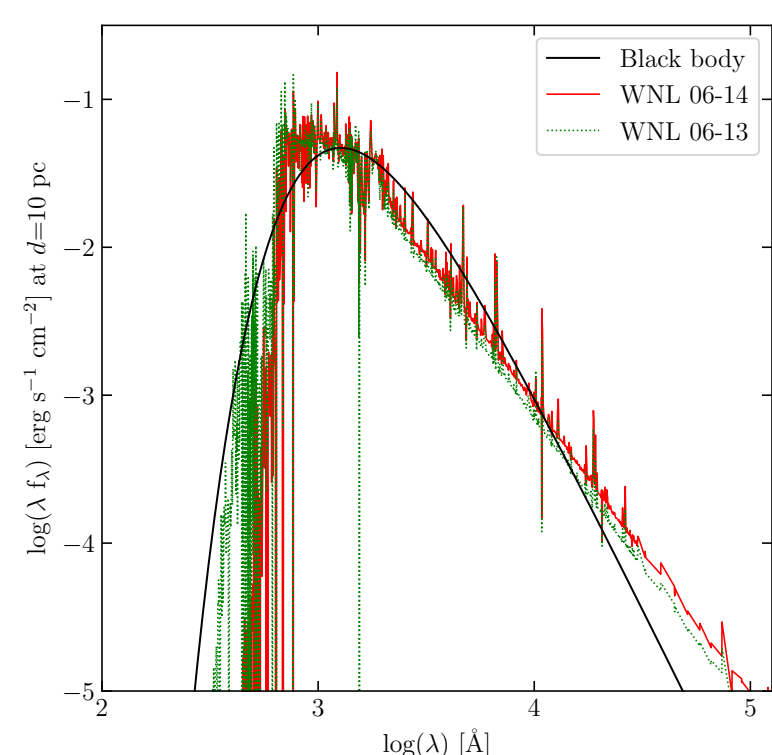


Fig 3. Comparison between black body ( $T_{\text{eff}}=28.8$  kK) emission and PoWR stellar atmosphere models. Solid red line: WNL 06-14 model ( $T_{\text{eff}}=28.8$  kK) and; dashed green line: WNL 06-13 ( $T_{\text{eff}}=32.1$  kK).

## Targets

We presented an analysis of the dust properties of the WR nebulae M1-67 and RCW 58 around WR 124 and WR 40, respectively. Upper panels of the Fig. 1 and Fig. 2 show multi-frequency images of these two nebulae.

### WR 124

Spectral type: WN8h  
Distance : 6.4 kpc  
Log  $\dot{M}$  :  $-4.3 M_{\odot} \text{ yr}^{-1}$   
 $v_{\infty}$  : 710 km s<sup>-1</sup>

### M1-67

Angular size:  $\sim 4'.3$

### WR 40

Spectral type: WN8h  
Distance : 3.8 kpc  
Log  $\dot{M}$  :  $-4.2 M_{\odot} \text{ yr}^{-1}$   
 $v_{\infty}$  : 650 km s<sup>-1</sup>

### RCW 58

Angular size:  $\sim 9' \times 8'$

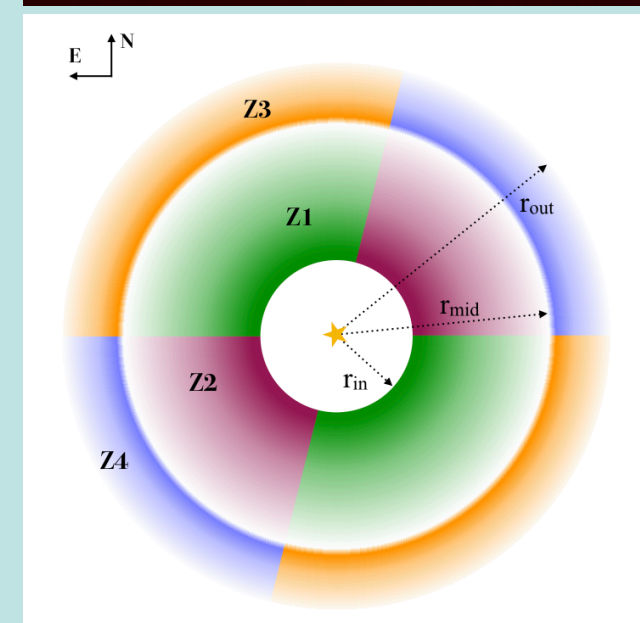
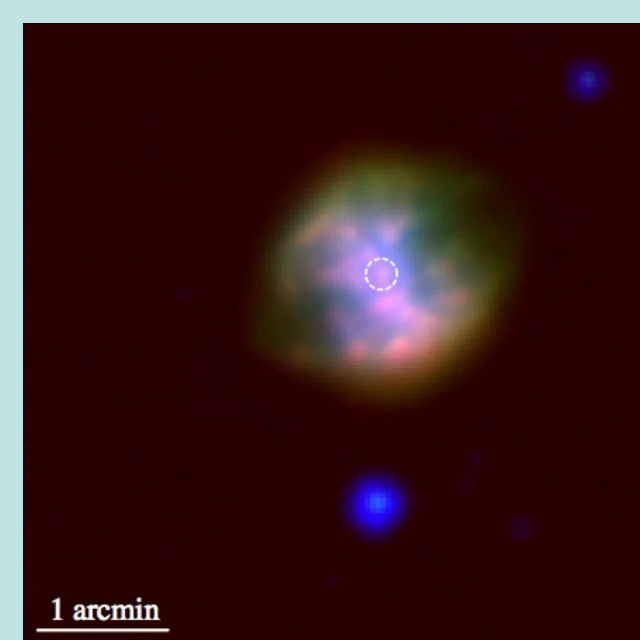


Fig 1. M1-67. Top: Color-composite IR image. North is up, east is left. Bottom: Schematic view of the distribution of gas (Z1, Z2, Z4) and dust (Z3) in our model (see [3]).

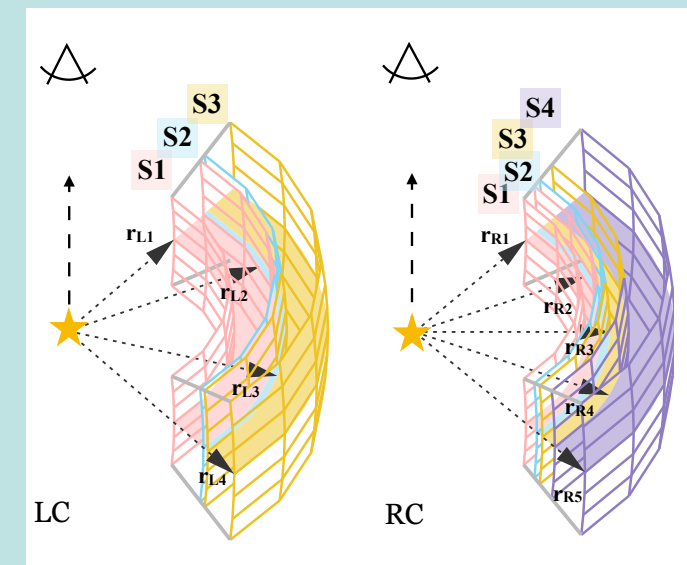
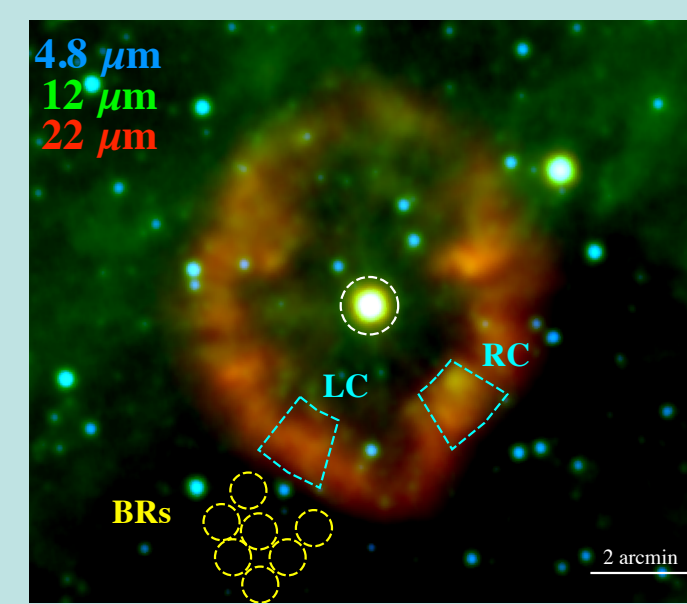


Fig 2. RCW 58. Top: Color-composite IR image. Cyan polygonal shapes indicate the selected regions for study (LC and RC). North is up, east is left. Bottom: Schematic view of the gas and dust distribution in the LC and RC clumps, on which our models are based (see [4]).

## Dust characteristics and spatial distribution

Multi-layer models were required to reproduce observational SED of M 1-67 and RCW 58 (see Fig. 4 and Fig. 5). A global model of RCW 58 is hampered by the extended background emission. For this reason, regions RC and LC have been modeled as representative of the properties of the ring nebula.

Schematic view of our models is shown in bottom panel of Fig. 1 and Fig. 2. From our models (see [3] and [4] for more detail):

1. We need an inner layer of pure gas and a dusty outer layer.
2. The dusty layer has two populations of dust, small ( $0.002 \mu\text{m} \leq a \leq 0.05 \mu\text{m}$ ) and big ( $0.6 \mu\text{m} \leq a \leq 0.9 \mu\text{m}$ ) grains.

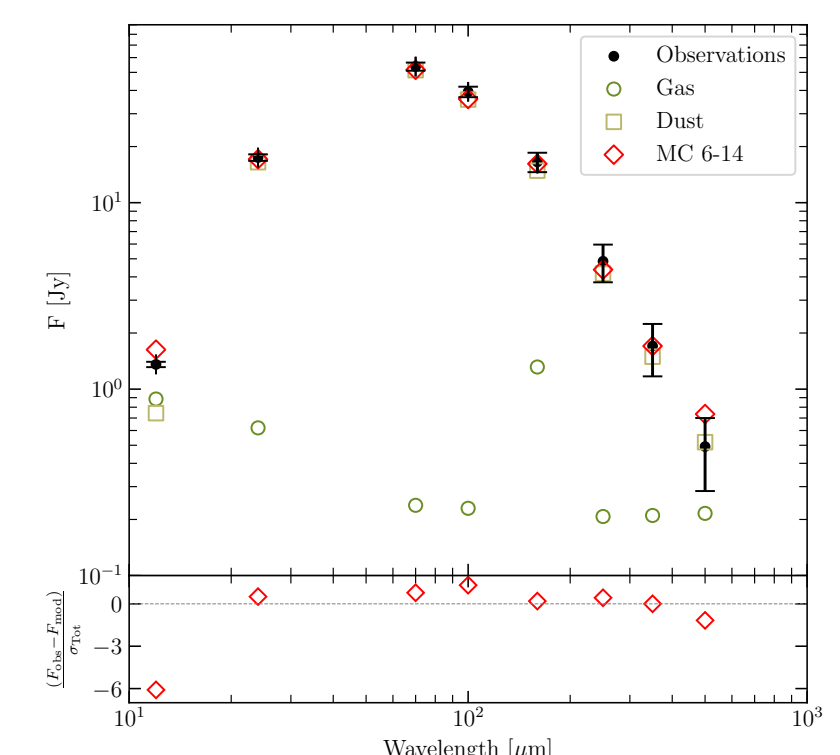


Fig 4. Observational SED of M1-67: black dots. The synthetic SED obtained from our model, MC 6-14: empty red diamonds.

## Observational constraints

1. We used the shape and flux of the IR spectral energy distribution (SED) to fit dust emission from our model. The IR SED was built from data corresponding to Spitzer, WISE and Herschel (and ATCA to the RCW 58 case) observations.
2. In order to calibrate the quantity of ionized gas we used the H $\alpha$  and H $\beta$  emission line fluxes and/or radio observations.

## Single or binary origin?

The maximum grain size of  $0.9 \mu\text{m}$  supports an eruptive formation [5] for M 1-67 and RCW 58. This is because mass-loss rates above  $\dot{M} > 10^{-3} M_{\odot} \text{ yr}^{-1}$  are required to shield the dust-formation region from stellar UV photons.

We estimated an initial mass for WR 124 and WR 40 (nebular mass calculated + current mass) around  $40 M_{\odot}$ , this rules out the possibility that the WR star had a LBV phase. On the other hand, the morphology and the dynamics of each nebula allows us to suggest dust formation through a CE ejection.

	M1-67	RCW 58
Morphology	Bipolar nebula	Torus pole-on nebula
Dynamics (Sirianni et al. 1998, Smith et al. 1988)	Ballistic clumps moving at $\sim 46 \text{ km s}^{-1}$	Clumping ring-like expanding structure at $30\text{-}87 \text{ km s}^{-1}$

CE evolution can lead to the ejection of the common envelope and a tighter binary (see Fig 6) [6]. Additionally, the presence of a compact object of WR 124 and WR 40 can be rule out because their dense stellar wind.

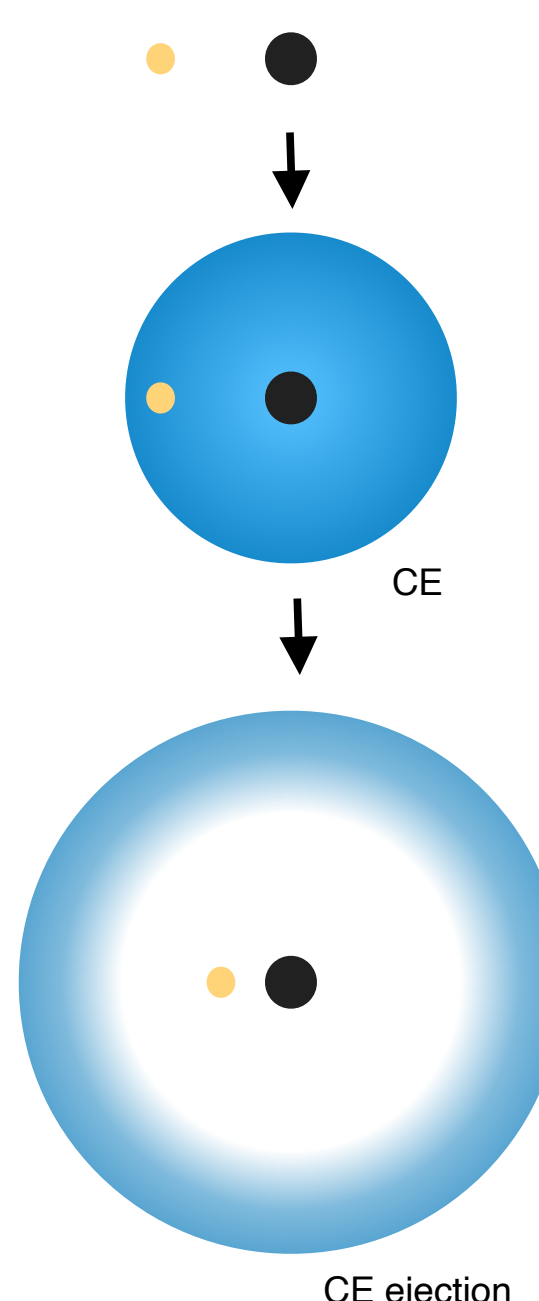


Fig 6. Illustration of a binary system evolution leading to a tighter binary and eventual CE ejection.

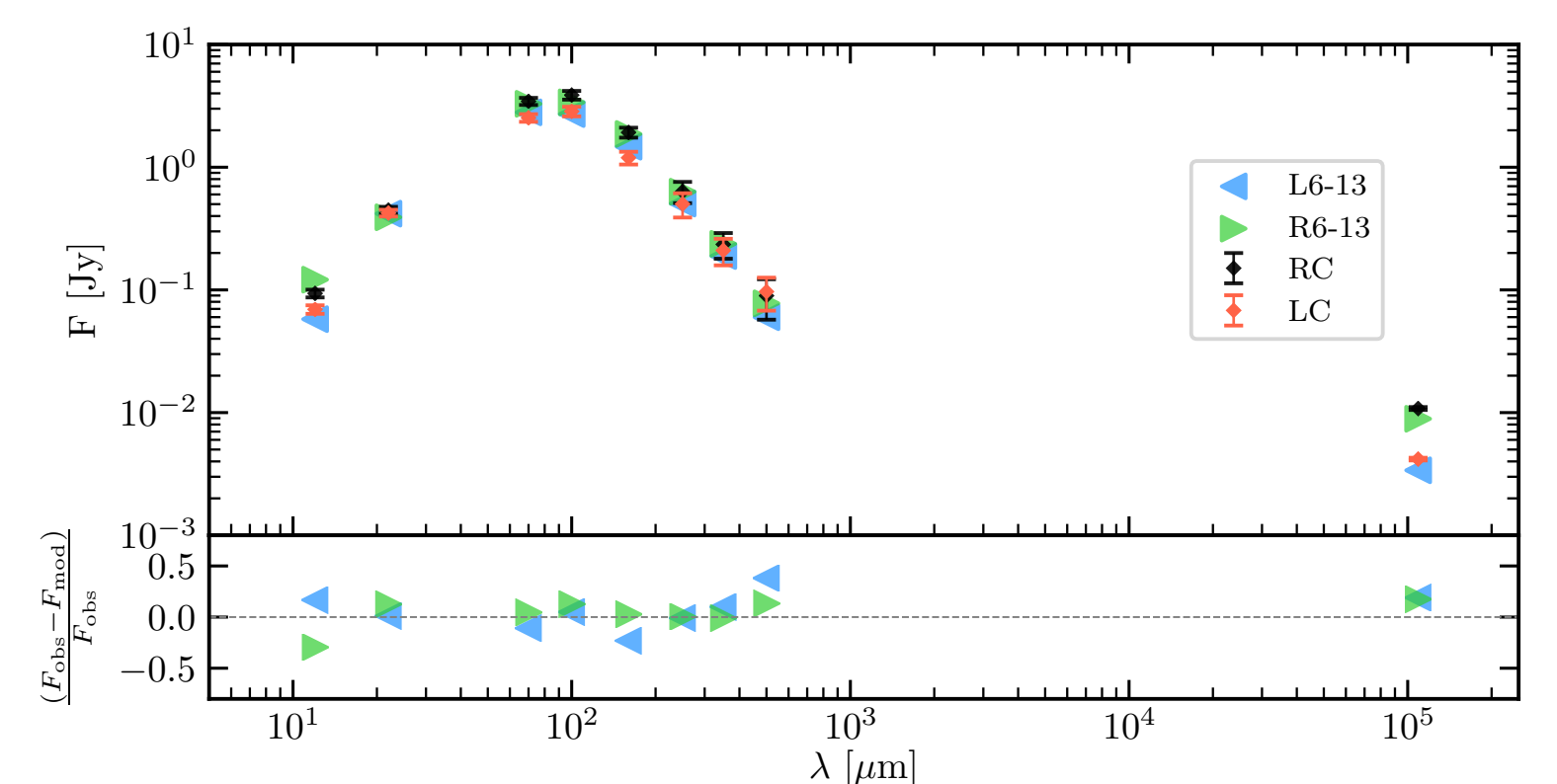


Fig 5. SED obtained from IR and ATCA observations of RCW 58: black and red diamonds correspond to RC and LC regions, respectively. The synthetic SED data points, obtained from best models of RC (R6-13) and LC (L6-13), are shown by triangles.

## To take home

We propose **M1-67 and RCW 58**, together with their progenitor stars, as the **first observational evidences of post-CE evolution in nebulae around massive stars**.

## References

- [1] Ferland, G., et al., 2013, RMxAA, 49, 137  
[2] Hamann, W.R., et al., 2006, A&A, 471, 1015  
[3] Jiménez-Hernández et al. 2020, MNRAS, 497, 4128

- [4] Jiménez-Hernández et al. 2021, MNRAS, 507, 3030  
[5] Kochanek C. S., 2011 ApJ, 743, 73  
[6] Ivanova N. et al. 2013, A&A Rev., 21, 59

## Acknowledgements

This research was supported by DGAPA-PAPIIT projects IA100720 and IN107019.